Chinese Journal of Aeronautics 25 (2012) 631-639

Contents lists available at ScienceDirect

Chinese Journal of Aeronautics

journal homepage: www.elsevier.com/locate/cja

Phase Residual Estimations for PCVs of Spaceborne GPS Receiver Antenna and Their Impacts on Precise Orbit Determination of GRACE Satellites

TU Jia, GU Defeng, WU Yi, YI Dongyun*

College of Science, National University of Defense Technology, Changsha 410073, China

Received 17 October 2011; revised 20 February 2012; accepted 11 April 2012

Abstract

In-flight phase center systematic errors of global positioning system (GPS) receiver antenna are the main restriction for improving the precision of precise orbit determination using dual-frequency GPS. Residual approach is one of the valid methods for in-flight calibration of GPS receiver antenna phase center variations (PCVs) from ground calibration. In this paper, followed by the correction model of spaceborne GPS receiver antenna phase center, ionosphere-free PCVs can be directly estimated by ionosphere-free carrier phase post-fit residuals of reduced dynamic orbit determination. By the data processing of gravity recovery and climate experiment (GRACE) satellites, the following conclusions are drawn. Firstly, the distributions of ionosphere-free carrier phase post-fit residuals from different periods have the similar systematic characteristics. Secondly, simulations show that the influence of phase residual estimations for ionosphere-free PCVs on orbit determination can reach the centimeter level. Finally, it is shown by in-flight data processing that phase residual estimations of current period could not only be used for the calibration for GPS receiver antenna phase center of foretime and current period, but also be used for the forecast of ionosphere-free PCVs in future period, and the accuracy of orbit determination can be well improved.

Keywords: global positioning system; precise orbit determination; phase center variations; phase residual estimation; GRACE

1. Introduction

Since spaceborne dual-frequency global positioning system (GPS) receiver was successfully applied in challenging minisatellite payload (CHAMP) mission [1-2], more and more low-earth orbit (LEO) satellite missions have been equipped with dual-frequency GPS receiver for precise navigation, such as gravity recovery and climate experiment (GRACE) mission [3-4], gravity field and steady-state ocean circulation explorer (GOCE) mission [5], TanDEM-X mission [6] and Korea multi-purpose satellite-5 (KOMPSAT-5) [7] mission. Due to the characteristic of broad time-space coverage, high precision and low cost, the spaceborne dual-frequency GPS receiver has become requisite equipment for LEO satellite. By the processing of GPS observation data, 3-dimensional (3D) in-flight position information of satellite can be obtained with a centimeter-level precision [8].

As the accuracy of final orbit and clock products for GPS satellites are continuously improved, orbit dynamical models for LEO satellite are well set up, the approaches of data processing and orbit determination are constantly advanced, the accuracy of obit determination based on dual-frequency GPS can be continuously improved and the error sources of GPS observation can be well separated. The noise level of GPS carrier phase measurement of GPS receiver can reach 1-2 mm and is much more accurate than GPS pseudo code observation. In order to fully exploit the accuracy for

*Corresponding author. Tel.: +86-731-84573260.
E-mail address: dongyun.yi@gmail.com
Foundation items: National Natural Science Foundation of China (61002033, 60902089); Open Research Fund of State Key Laboratory of Astronautic Dynamics of China (2011ADL-DW0103)

1000-9361
doi:10.1016/S1000-9361(11)60428-7

precise orbit determination (POD), the carrier phase observation data has a dominant influence. The reduced dynamic orbit determination method [9-11] is widely used nowadays, which combines the geometric strength of the GPS observations with the orbit dynamical model constraints. In this way, the available accuracy of the GPS measurements may be fully exploited without sacrificing the robustness offered by dynamic orbit determination techniques. Meanwhile, the in-flight systematic deviation of GPS receiver antenna phase center has become the main influence on orbit determination, which is mainly caused by the ground fixing error of GPS receiver antenna, the vibration of the satellite launch and near-field multipath, etc. Therefore, the research on in-flight calibration for phase center of GPS receiver antenna [12-16] provides a valid way to further improve the precision of orbit determination.

The residual approach [12-16], is one of the widely used methods for in-flight calibration of GPS receiver antenna phase center variations (PCVs). In this approach, in-flight calibration is derived from carrier phase post-fit residuals of orbit determination taking into account the nominal phase center offset (PCO) and PCVs from the ground calibration [12-13]. Some scholars have studied this approach. The JASON-1 orbits [14] have already been successfully improved by this approach. Meanwhile, the Jet Propulsion Laboratory (JPL) [15] applies this approach to the GRACE satellites, which serves as primary data source to derive PCVs for the GPS transmitter antennas. In addition, Montenbruck [12], Jäggi [13] and Bock [16], et al. use this approach to calibrate the PCVs of GPS receiver antennas onboard GRACE satellites, TerraSAR-X and GOCE, respectively.

Subsequently we mainly focus on the phase residual estimations for ionosphere-free PCVs based on GPS carrier phase observation model. Followed by the correction model of spaceborne GPS receiver antenna phase center, ionosphere-free PCVs can be directly estimated by ionosphere-free carrier phase post-fit residuals of reduced dynamic orbit determination, which can be exhibited in the form of phase residual pattern and added to the orbit determination again. By the in-flight GPS data processing of GRACE satellites, phase residual patterns of three periods will be produced at first. Then the similar distribution characteristics of the phase residual patterns from different periods will be validated and the phase residual estimations of middle period will be selected as the final estimations for ionosphere-free PCVs. At last, the impacts of phase residual estimations on orbit determination will be analyzed by simulations and in-flight data processing.

2. Phase Residual Estimations for PCVs of Spaceborne Dual-frequency GPS Receiver Antenna

When observed by spaceborne dual-frequency GPS, the real measurement is the geometry distance between the antenna phase center position of the GPS receiver and the GPS satellite at the moment of signal reception and transmission, respectively. Therefore, in order to realize high-precision orbit determination of LEO satellite using dual-frequency GPS, the determination of GPS receiver antenna phase center position is momentous.

2.1. Observation equation

In order to eliminate the first order ionosphere delay, dual-frequency ionosphere-free combination observations are always adopted. For the pseudo code and carrier phase observations, the ionosphere-free combination yields

$$P_{\mathrm{IF}}^{j}(t)=\frac{f_1^2}{f_1^2-f_2^2}P_1^j(t)-\frac{f_2^2}{f_1^2-f_2^2}P_2^j(t)=\rho^j(t,\tau^j)+c\delta t(t)+\delta\rho_{\mathrm{cor}}(t)+\varepsilon_{P_{\mathrm{IF}}}^j(t) \quad (1)$$

$$L_{\mathrm{IF}}^{j}(t)=\frac{f_1^2}{f_1^2-f_2^2}L_1^j(t)-\frac{f_2^2}{f_1^2-f_2^2}L_2^j(t)=\rho^j(t,\tau^j)+c\delta t(t)+b_{\mathrm{IF}}^j+\delta\rho_{\mathrm{cor}}(t)+\varepsilon_{L_{\mathrm{IF}}}^j(t) \quad (2)$$

where subscript "IF" denotes ionosphere-free combination, subscripts "1" and "2" denote different frequencies, subscript "*j*" denotes the *j*th GPS satellite, P_{IF} pseudo code ionosphere-free combination, L_{IF} phase ionosphere-free combination, P code observation, L phase observation, f_i (i=1, 2) the carrier frequency, τ^j the real signal travelling time from GPS satellite j to LEO satellite which can be obtained by iterative calculation, $\rho^j(t, \tau^j)$ the geometric distance between the mass center position of GPS satellite j and LEO satellite at signal transmission epoch $t-\tau^j$ and signal reception epoch t respectively, c light velocity, δt the clock offset of LEO satellite, b_{IF} the ambiguity of phase ionosphere-free combination, $\varepsilon_{P_{\mathrm{IF}}}$ and $\varepsilon_{L_{\mathrm{IF}}}$ contain thermal measurement noise, multipath, and all other unmodeled errors, and $\delta\rho_{\mathrm{cor}}$ is a series of corrections which can be denoted as

$$\delta\rho_{\mathrm{cor}}(t)=-c\delta\rho_{\mathrm{clk}}(t,\tau^j)+\delta\rho_{\mathrm{rel}}(t)+\delta\rho_{\mathrm{GPS}}^j(t)+\delta\rho_{\mathrm{LEO,IF}}(t) \quad (3)$$

where $\delta\rho_{\mathrm{clk}}$ is the clock correction of GPS satellite j at epoch $t-\tau^j$, $\delta\rho_{\mathrm{rel}}$ the relativity correction of GPS satellite j, $\delta\rho_{\mathrm{GPS}}^j$ the phase center offset correction of GPS satellite j, and $\delta\rho_{\mathrm{LEO,IF}}$ the ionosphere-free phase center correction of LEO satellite. $\delta\rho_{\mathrm{clk}}$, $\delta\rho_{\mathrm{rel}}$, and $\delta\rho_{\mathrm{GPS}}$ have been studied in Ref. [17]. In this paper, only the ionosphere-free phase center correction of LEO satellite, $\delta\rho_{\mathrm{LEO,IF}}$, will be analyzed in detail.

For convenience, $\rho^j(t, \tau^j)$ has to be linearized as

$$\rho^j(t,\tau^j)=\rho_0^j(t,\tau^j)-(\boldsymbol{e}^j(t))^{\mathrm{T}}\cdot\Delta\boldsymbol{r}(t) \quad (4)$$

where

$$\rho_0^j(t,\tau^j)=\|\boldsymbol{r}^j(t-\tau^j)-\boldsymbol{r}_0(t)\| \quad (5)$$

$$\Delta\boldsymbol{r}(t)=\boldsymbol{r}(t)-\boldsymbol{r}_0(t) \quad (6)$$

$$\boldsymbol{e}^j(t)=\frac{\boldsymbol{r}^j(t-\tau^j)-\boldsymbol{r}_0(t)}{\|\boldsymbol{r}^j(t-\tau^j)-\boldsymbol{r}_0(t)\|} \quad (7)$$

where $\boldsymbol{r}^j(t-\tau^j)$ is the mass center position of GPS satellite j in conventional inertial reference frame (CIRF) at epoch $t-\tau^j$, $\boldsymbol{r}_0(t)$ the approximate mass center position of LEO satellite in CIRF, and $\boldsymbol{e}^j(t)$ a line of sight (LOS) vector.

2.2. Correction model of spaceborne GPS receiver antenna phase center

In ideal circumstances, the phase center of GPS receiver antenna is defined as the center of wave front in radiation field. But in practice, the wave front will fluctuate caused by the characteristic of antenna and machining art, etc, and the locations of every signal reception do not overlap [18]. Therefore, GPS receiver antenna phase center is the instantaneous location where the GPS signal is actually received.

For the convenience of description, the definition of antenna-fixed coordinate system (AFCS) [12] is given at first. The origin o is mechanical antenna reference point (ARP). The positive z axis coincides with the mechanical symmetry axis and points along the boresight direction. The y axis and x axis point from the mechanical ARP into the respective directions, which depend on the specific mounting of the antennas. Take AFCS of GRACE satellites for instance. The x axis of AFCS coincides with X axis of satellite body coordinate system (SBCS). The y axis of AFCS is in the opposite direction with Y axis of SBCS and z axis of AFCS completing a right-handed coordinate system. In AFCS, the azimuth angle of a vector $\boldsymbol{r}$ is defined as an angle between the projection of $\boldsymbol{r}$ in xoy plane and positive x axis and is counted in a counter-clockwise sense from x axis to y axis. The elevation angle of a vector $\boldsymbol{r}$ is defined as an angle between $\boldsymbol{r}$ and xoy plane.

In AFCS, the phase center of GPS receiver antenna consists of a PCO vector and PCVs [12-13]. The PCO vector $\boldsymbol{r}_{\mathrm{PCO}}$ describes the difference between the mean center of the wave front and the ARP. PCVs represent direction-dependent distortions of the wave front, which can be modeled as a consistent function φ that depends on azimuth and elevation of the observation from the position indicated by the PCO vector, i.e., the LOS vector $\boldsymbol{e}$. Assuming that the ARP vector in SBCS is $\boldsymbol{r}_{\mathrm{ARP}}$ and the LOS vector in CIRF is $\boldsymbol{e}^j$, the phase center correction of GPS receiver antenna on L_i (i = 1, 2) band can be given as

$$\delta\rho_{\mathrm{LEO},i}(\boldsymbol{e}^j)=\delta\rho_{\mathrm{ARP}}(\boldsymbol{e}^j)+\delta\rho_{\mathrm{PCO},i}(\boldsymbol{e}^j)+\varphi_i(\boldsymbol{e}^j) \quad (8)$$

where

$$\delta\rho_{\mathrm{ARP}}(\boldsymbol{e}^j)=-(\boldsymbol{e}^j(t))^{\mathrm{T}}\cdot\boldsymbol{M}_{\mathrm{SBCS\_CIRF}}\cdot\boldsymbol{r}_{\mathrm{ARP}} \quad (9)$$

$$\delta\rho_{\mathrm{PCO},i}(\boldsymbol{e}^j)=-(\boldsymbol{e}^j(t))^{\mathrm{T}}\cdot\boldsymbol{M}_{\mathrm{AFCS\_CIRF}}\cdot\boldsymbol{r}_{\mathrm{PCO},i} \quad (10)$$

where $\boldsymbol{M}_{\mathrm{SBCS\_CIRF}}$ is a transformation matrix from SBCS to CIRF, and $\boldsymbol{M}_{\mathrm{AFCS\_CIRF}}$ a transformation matrix from AFCS to CIRF.

From Eqs. (8)-(10), the ionosphere-free correction of phase center can be expressed as

$$\delta\rho_{\mathrm{LEO,IF}}(\boldsymbol{e}^j)=\frac{f_1^2}{f_1^2-f_2^2}\delta\rho_{\mathrm{LEO},1}(\boldsymbol{e}^j)-\frac{f_2^2}{f_1^2-f_2^2}\delta\rho_{\mathrm{LEO},2}(\boldsymbol{e}^j)=\delta\rho_{\mathrm{ARP}}(\boldsymbol{e}^j)+\delta\rho_{\mathrm{PCO,IF}}(\boldsymbol{e}^j)+\varphi_{\mathrm{IF}}(\boldsymbol{e}^j) \quad (11)$$

2.3. Phase residual estimations for ionosphere-free PCVs

The PCO vector and PCVs can be obtained from ground calibration [12]. But such a nominal antenna calibration result does not reflect the influence of error sources which are additionally encountered in the actual spacecraft environment, e.g., the influence of near-field multipath. The in-flight phase center locations are different from ground calibration result. For precise orbit determination, this deviation cannot be neglected. From Eq. (8) and Eq. (10), we can see that the increment $\Delta\boldsymbol{r}_{\mathrm{PCO},i}$ of the PCO vector can be absorbed by PCVs. Therefore, the PCO vector is still selected as the ground calibration result and only the PCVs are estimated in actual spacecraft environment.

Only considering $\delta\rho_{\mathrm{ARP}}$ and $\delta\rho_{\mathrm{PCO,IF}}$ and omitting φ_{IF} in Eq. (11), Eq. (11) is substituted into Eq. (2). Assuming that the GPS ionosphere-free carrier phase observation value in epoch t is $z_{\mathrm{IF}}^j(t)$, then we can get

$$\varphi_{\mathrm{IF}}(\boldsymbol{e}^j)\approx z_{\mathrm{IF}}^j(t)-L_{\mathrm{IF}}^j(t) \quad (12)$$

From Eq. (12), the ionosphere-free PCVs can be directly estimated by the post-fit residuals of orbit determination. As a result of relatively lower precision of pseudo code, only the ionosphere-free carrier phase post-fit residuals of reduced dynamic orbit determination are used to estimate the ionosphere-free PCVs.

In this study, the ionosphere-free carrier phase post-fit residuals are sorted in azimuth/elevation bins of $\Delta A\times\Delta E$. In the region of $[(n-1)\Delta A, n\Delta A)]\times[(m-1)\Delta E, m\Delta E]$, ($n$ = 1, 2, $\cdots$, $360/\Delta A$; m = 1, 2, $\cdots$, $90/\Delta E$), the estimation for ionosphere-free PCV is the mean value of all the ionosphere-free carrier phase post-fit residuals fallen into this region. The values of ΔA and ΔE are both selected as 5° in this paper and the phase residual estimations for ionosphere-free PCVs are exhibited in the form of phase residual pattern.

3. Numerical Analysis for GRACE Satellites

3.1. Data sets and processing strategy

The GRACE mission [3], launched on March 17, 2002, is a joint partnership between the National Aeronautics and Space Administration (NASA) in the United States and Deutsches Zentrum für Luft- und Raumfahrt (DLR) in Germany. It consists of two identical formation flying spacecraft (GRACE *A* and GRACE *B*) in a near polar, near circular orbit with an initial altitude of about 500 km. The spacecraft have a nominal separation of 220 km. The key science instruments [19] onboard both spacecraft include a BlackJack GPS receiver, a SuperSTAR accelerometer, a star tracker, a K-band ranging (KBR) system and a satellite laser ranging (SLR) retro-reflector. The BlackJack GPS receiver exhibits a representative noise level of 1 mm for L_1 and L_2 carrier phase measurements.

The data sets used here include GPS observation data (GPS1B), spacecraft attitude data (SCA1B), KBR data (KBR1B), precise science orbit data (GNV1B) of GRACE *A* and GRACE *B* from GeoForschungsZentrum (GFZ) [20], the final GPS orbits and the 30 s high-rate satellite clock corrections from the Center for Orbit Determination in Europe (CODE) [21]. The data cover the periods from October 31 to November 13 of 2004 and from January 1 to January 28 of 2006. The PCOs of GPS receiver antennas onboard GRACE satellites [22] in respective SBCS are listed in Table 1.

Table 1 PCOs of GPS receiver antennas onboard GR- ACE satellites in the respective SBCS

GRACE	*X*/m	*Y*/m	*Z*/m
A	0.000 4	− 0.000 4	− 0.414 0
B	0.000 6	− 0.000 8	− 0.414 3

The LEO orbit determination is implemented in the separate software tools as part of the National University of Defense Technology (NUDT) Orbit Determination Software 1.0. The GPS observation data processing consists of GPS observation data preprocessing [17], reduced dynamic orbit determination with medium precision [17, 22], GPS observation data editing [17, 22] and reduced dynamic orbit determination with high precision. Both reduced dynamic orbit determinations with medium and high precision make use of zero-difference reduced dynamic batch least-squares approach. In this approach, the individual spacecraft positions at each measurement epoch are replaced by the spacecraft trajectory model in Eq. (1) and Eq. (2). We make use of known physical models of the spacecraft motion to constrain the resulting position estimates and introduce three empirical acceleration components to absorb all other unmodeled perturbation. As the atmospheric density and solar activity are difficult to model accurately, atmospheric drag coefficient and solar radiation pressure coefficient in the models of solar radiation pressure and atmospheric drag are also estimated. The orbit dynamical models and reference frames used for reduced dynamic orbit determination are listed in Table 2.

Table 2 Overview of dynamical models and reference frames used for reduced dynamic orbit determination

Item	Description
Static gravity field	GGM02C 150×150 [23]
Solid Earth tide	IERS96, 4×4 [24]
Polar tide	IERS96 [24]
Ocean tide	CSR4.0
3rd body gravity	Sun and moon
Solar radiation pressure	Ball model, conical earth shadow, solar radiation press coefficient C_R is estimated [25]
Atmospheric drag	Jacchia 71density model (NOAA solar flux (daily) and geomagnetic activity (3 hourly)), atmospheric drag coefficient C_D is estimated [25]
Relativity	Schwarzschild
Precession	IAU1976 [24]
Nutation	IAU1980 + EOPC correction [24]
Earth orientation	EOPC04
Solar ephemerides	JPL DE405
Terrestrial reference frame	International terrestrial reference frame (ITRF) 2000 [26]
Conventional inertial reference frame	J2000.0 [27]

Three empirical acceleration components in directions of radial (R), transverse (T) and normal (N) are denoted as [28]

$$\boldsymbol{a}_{\mathrm{RTN}} = \begin{bmatrix} c_{\mathrm{R}} \cos u + s_{\mathrm{R}} \sin u \\ c_{\mathrm{T}} \cos u + s_{\mathrm{T}} \sin u \\ c_{\mathrm{N}} \cos u + s_{\mathrm{N}} \sin u \end{bmatrix} \begin{bmatrix} \boldsymbol{e}_{\mathrm{R}} \\ \boldsymbol{e}_{\mathrm{T}} \\ \boldsymbol{e}_{\mathrm{N}} \end{bmatrix} \tag{13}$$

where u is satellite latitude, c_R, s_R, c_T, s_T, c_N and s_N are empirical acceleration coefficients, $\boldsymbol{e}_R$, $\boldsymbol{e}_T$ and $\boldsymbol{e}_N$ are unit vectors in directions of R, T, and N, which are three axes of RTN coordinate system.

All the parameters are estimated by batch least-squares approach [17, 22]. The parameters estimated in orbit determination are listed in Table 3.

Table 3 Parameters estimated in orbit determination

Estimated parameter	Description
Initial state vector	3D position and velocity estimated per day
Atmospheric drag coefficient	Estimated per 3 hours
Solar radiation pressure coefficient	Estimated per 12 hours
Empirical acceleration coefficient	c_T, s_T, c_N, s_N estimated per orbital revolution
LEO clock offset	Estimated epoch-wise
Ambiguity	Estimated per arc of continuous tracking of a single GPS satellite

Orbit determination process is typically conducted in 24 h data batches and Adams-Cowell multi-step inte-

gration method [29] is used for orbit integration.

3.2. Generation of phase residual patterns

At first, all the GPS observation data of GRACE *A* and GRACE *B* are directly used to determine the precise orbits by reduced dynamic orbit determination approach. The ionosphere-free carrier phase post-fit residuals are stored in three periods. The first period is from October 31 to November 13 of 2004. The second period is from January 1 to January 14 of 2006. The third period is from January 15 to January 28 of 2006. The ionosphere-free carrier phase residual patterns of three periods for GRACE satellites are given in Fig. 1.

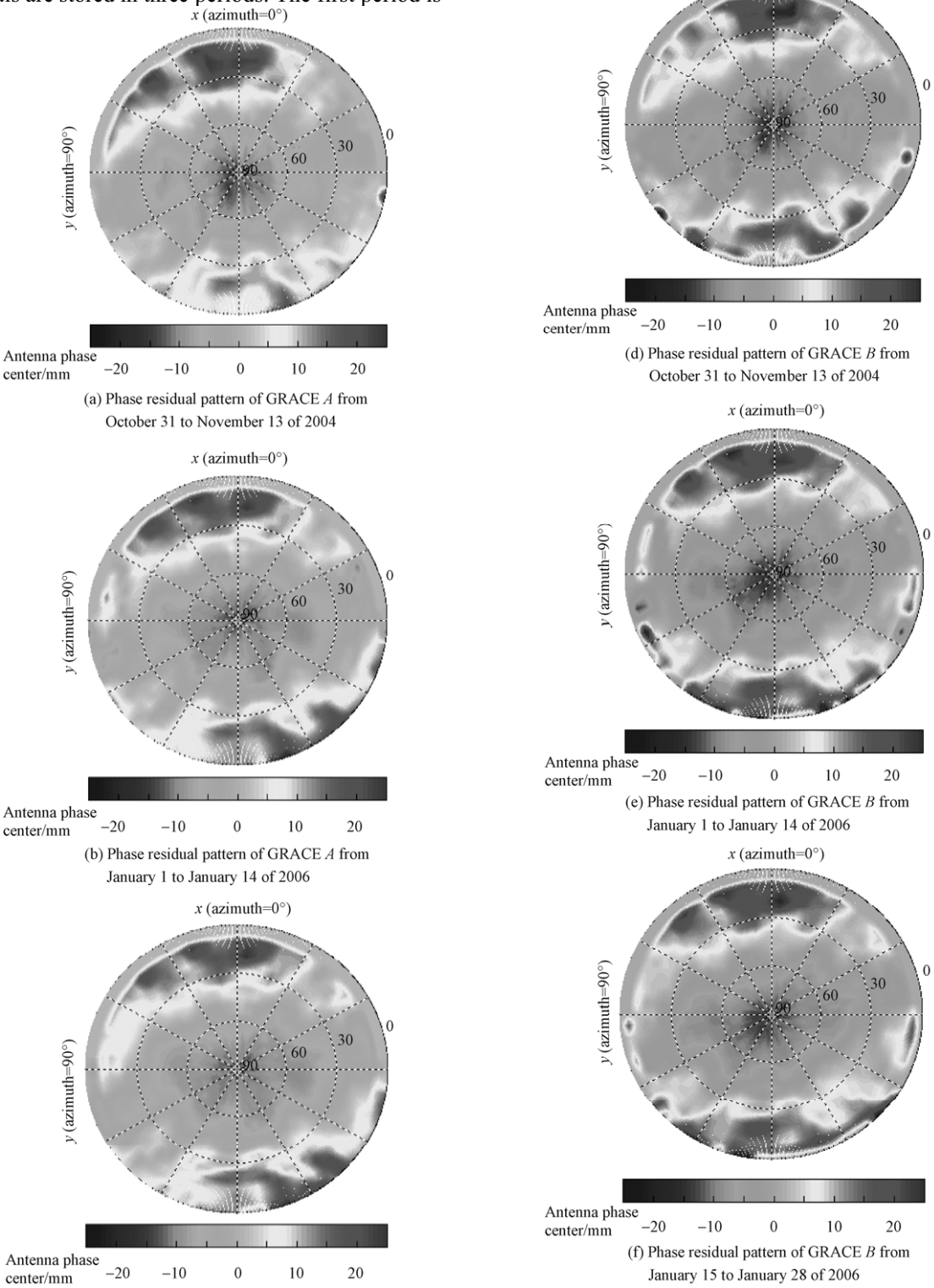

(a) Phase residual pattern of GRACE *A* from October 31 to November 13 of 2004

(b) Phase residual pattern of GRACE *A* from January 1 to January 14 of 2006

(c) Phase residual pattern of GRACE *A* from January 15 to January 28 of 2006

(d) Phase residual pattern of GRACE *B* from October 31 to November 13 of 2004

(e) Phase residual pattern of GRACE *B* from January 1 to January 14 of 2006

(f) Phase residual pattern of GRACE *B* from January 15 to January 28 of 2006

Fig. 1 Ionosphere-free carrier phase residual patterns of three periods for GRACE *A* and GRACE *B*.

Figure 1 shows that the distributions of ionosphere-free carrier phase post-fit residuals from three periods for single GRACE satellite keep fixed and exhibit the similar systematic error characteristics. Based on these characteristics, the phase residual estimations of the middle period, i.e., the period from January 1 to January 14 of 2006, are selected as the final estimations for ionosphere-free PCVs. In addition, it is also shown by Fig. 1 that the ionosphere-free carrier phase post-fit residuals are close to 0 m in the direction of *y* axis in AFCS and it is just because that PCVs perpendicular to the flight direction are to some extent absorbed by the parameters of LEO clock offsets and carrier phase ambiguities.

3.3. Simulation study

The simulations are conducted to assess the changes of orbit determination introduced only by phase residual estimations for ionosphere-free PCVs. The initial states of GRACE satellites at 00:00:00 on January 2, 2006 in J2000.0 inertial reference frame are listed in Table 4. The PCOs of both GRACE satellites are listed in Table 1. The GPS orbits from the final products of the CODE analysis center and numerically integrated dynamic GRACE orbits served as the true GPS orbits and the true GRACE orbits to generate the 24 h simulated GPS observations. All the dynamical models listed in Table 2 are considered.

Table 4 Initial states of GRACE satellites in J2000.0 inertial system at 00:00:00 on January 2, 2006

GRACE	Position			Velocity		
	x/m	*y*/m	*z*/m	V_x/(m·s^{-1})	V_y/(m·s^{-1})	V_z/(m·s^{-1})
A	4 032 811.318 646	−704 790.431 146	5 493 466.057 718	6 062.967 061	−842.247 917	− 4 541.059 971
B	4 144 386.925 409	−720 031.189 719	5 408 710.165 685	5 969.636 585	−825.667 565	− 4 665.027 569

The phase residual estimations for ionosphere-free PCVs of middle period are added to the process of orbit determination, and the parameters listed in Table 3 are estimated. The reduced dynamic orbit solutions are compared with the reference orbits obtained directly by orbit integral from initial states in RTN coordinate system (see Fig. 2).

The root mean square (RMS) values of R, T and N position components for GRACE *A* are 0.004 9, 0.010 6, 0.003 8 m, and the 3D RMS value is 0.012 3 m, while the RMS values of R, T, N position components for GRACE *B* are 0.003 9, 0.008 7, 0.004 7 m, and 3D RMS value is 0.010 6 m. It is shown by these orbit comparison results that the influence of phase residual estimations for ionosphere-free PCVs on orbit determination of GRACE satellites can reach the centimeter level.

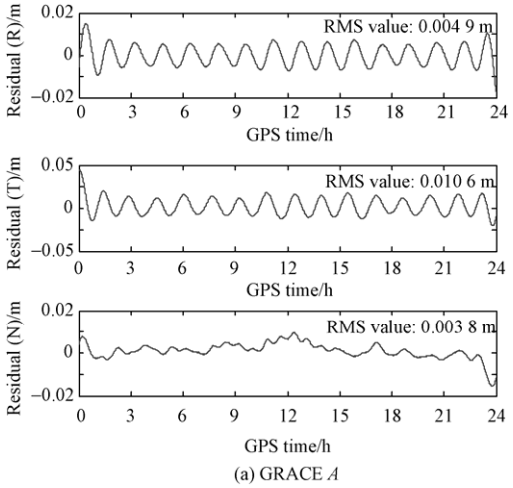

(a) GRACE *A*

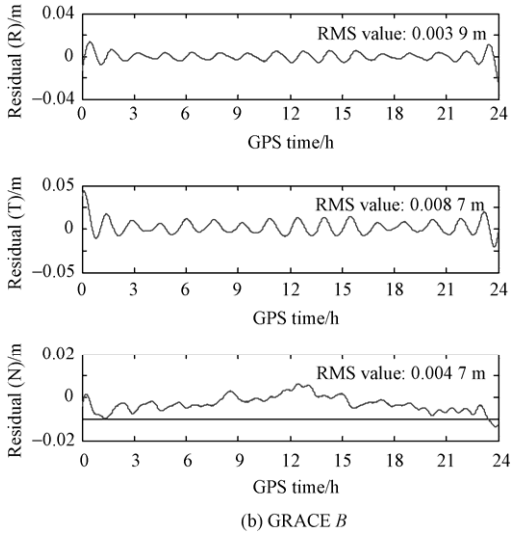

(b) GRACE *B*

Fig. 2 Comparison between reference orbits and reduced dynamic orbit solutions adding phase residual estimation for GRACE simulation data.

3.4. In-flight data analysis

The phase residual estimations for ionosphere-free PCVs of middle period are added to orbit determination process for all the GPS observation data of GRACE satellites from three periods. The impacts of phase residual estimations for ionosphere-free PCVs on orbit determination are analyzed by internal and external validations.

3.4.1 Internal validation

The internal validation of orbit solutions is provided

by the ionosphere-free carrier phase post-fit residuals of reduced dynamic orbit determination approach, which can be used to measure the consistency of the applied models with the GPS observation data. The ionosphere-free carrier phase post-fit residuals are stored in three periods as aforementioned and the statistic results are shown in Table 5.

It is found by statistic process that the mean values of ionosphere-free carrier phase post-fit residuals are close to 0 m. Table 5 shows that as the phase residual estimations for ionosphere-free PCVs are added to orbit determination, not only the ionosphere-free carrier phase post-fit residuals of middle period are obviously reduced, but those of other two periods are also obviously reduced. It is illuminated that the applied models and the GPS observation data are in better consistency after adding phase residual estimations for ionosphere-free PCVs.

Table 5 RMS values of ionosphere-free carrier phase post-fit residuals for orbit determination

Period	RMS value/m			
	GRACE *A*		GRACE *B*	
	Direct orbit determination	Adding phase residual estimation	Direct orbit determination	Adding phase residual estimation
2004-10-31 to 2004-11-13	0.013 3	0.011 0	0.012 2	0.009 6
2006-01-01 to 2006-01-14	0.013 6	0.010 8	0.012 7	0.009 6
2006-01-15 to 2006-01-28	0.013 1	0.010 4	0.012 1	0.009 1
Mean value of all periods	0.013 3	0.010 7	0.012 3	0.009 4

3.4.2 External validation

Orbit comparison with JPL precise science orbit and relative position validation by KBR data is selected as external validation.

1) Orbit comparison

JPL precise science orbit is created by processing zero-difference ionosphere-free pseudo code and carrier phase data with the GIPSY-OASIS software package, which is distributed along with the GRACE GPS data and is a part of GRACE Level 1B product. The differences between the orbits obtained in this paper and the JPL precise science orbit are computed in the R, T and N directions at the discrete epoch (see Fig. 3). The RMS values of orbit comparisons for three periods are listed in Table 6.

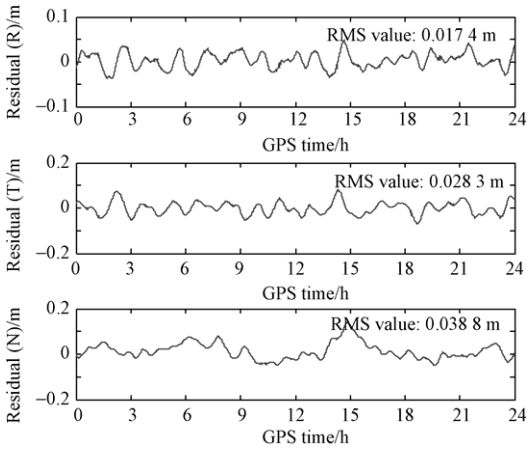

Fig. 3 Comparison between JPL precise science orbit and reduced dynamic orbit solution adding phase residual estimation for GRACE *A* on January 5, 2006.

Table 6 RMS values for GRACE satellites orbit comparison between reduced dynamic orbit solutions and JPL precise science orbit

Period	Phase residual estimation	RMS value / m							
		GRACE *A*				GRACE *B*			
		R	T	N	3D	R	T	N	3D
2004-10-31 to 2004-11-13	No adding	0.027 7	0.044 3	0.044 3	0.068 5	0.027 2	0.043 6	0.040 4	0.065 4
	Adding	0.025 5	0.039 1	0.041 0	0.062 1	0.025 4	0.040 2	0.038 3	0.061 1
2006-01-01 to 2006-01-14	No adding	0.020 2	0.033 9	0.039 3	0.055 7	0.018 9	0.030 6	0.040 7	0.054 3
	Adding	0.017 8	0.030 1	0.040 6	0.053 6	0.016 7	0.028 6	0.041 5	0.053 1
2006-01-15 to 2006-01-28	No adding	0.018 9	0.034 9	0.036 4	0.053 8	0.016 6	0.029 0	0.035 5	0.048 7
	Adding	0.016 5	0.030 9	0.037 0	0.050 9	0.015 2	0.027 2	0.036 5	0.047 9
Mean value of all periods	No adding	0.022 6	0.038 0	0.040 1	0.059 7	0.021 4	0.035 0	0.038 9	0.056 6
	Adding	0.020 3	0.033 6	0.039 5	0.055 7	0.019 6	0.032 5	0.038 8	0.054 3

In Table 6, it is shown that all the orbit determination accuracy of three periods is improved by adding phase residual estimations of middle period. In all periods, the 3D RMS value of orbit comparison results is reduced from 0.059 7 m to 0.055 7 m for GRACE *A* and from 0.056 6 m to 0.054 3 m for GRACE *B*, and the accuracy of each direction is improved for both satellites. These results manifest that the phase residual estimations for ionosphere-free PCVs of current period can not only be used for the calibration of the previous and current periods, but also be used to forecast the ionosphere-free PCVs of future period, and the accuracy can be well improved. In addition, orbit determination accuracy of R and T components can be obviously improved, but the accuracy improvements in N direction are not so obvious. It is mainly because the N direction of RTN coordinate system corresponds to the *y* axis of AFCS and the values of phase residual esti-

mations (see Fig. 1) along this direction are close to 0 m, so the accuracy improvements of orbit in this direction are not so obvious.

2) Orbit validation with KBR data

KBR system is one of the key scientific instruments onboard the GRACE satellites, which measures the one-way range change between the twin GRACE satellites with a precision of about 10 μm for KBR range at a 5 s data interval. As the high precision of KBR data, the relative orbit accuracy of the GRACE satellites can be validated.

The relative positions obtained by orbit determination solutions and JPL precise science orbit are validated by KBR data respectively, and the KBR comparison results are shown in Table 7.

Table 7 shows that the improvements of relative position accuracy are obvious by adding phase residual estimations of middle period. The accuracy of all periods is improved by 0.002 6 m and is comparable to relative position accuracy of JPL precise science orbit. By adding the phase residual estimations, the phase systematic deviations of both satellites can be removed, and relative position accuracy can be obviously improved.

Table 7 Standard deviations of KBR validation residuals

Period	Standard deviation/m		
	Direct orbit determination	Adding phase residual estimation	JPL precise science orbit
2004-10-31 to 2004-11-13	0.021 1	0.018 6	0.017 0
2006-01-01 to 2006-01-14	0.015 7	0.013 1	0.013 5
2006-01-15 to 2006-01-28	0.018 1	0.015 2	0.015 2
Mean value of all periods	0.018 4	0.015 8	0.015 3

4. Conclusions

1) Phase residual estimations for ionosphere-free PCVs are studied in this paper. By the direct processing of reduced dynamic orbit determination for GRACE satellites, the ionosphere-free carrier phase post-fit residuals on phase residual patterns from three periods have the similar distributions.

2) By the simulations of GRACE satellites, the impacts of phase residual estimations for ionosphere-free PCVs on orbit determination in R, T and N directions are 0.004 9, 0.010 6, 0.003 8, 0.012 3 m of 3D for GRACE *A*, and 0.003 9, 0.008 7, 0.004 7, 0.010 6 m of 3D for GRACE *B*. Therefore, the influence of phase residual estimations for ionosphere-free PCVs can reach the centimeter level.

3) According to the internal validation results, as the phase residual estimations of middle period are added to orbit determination, not only the ionosphere-free carrier phase post-fit residuals of middle period, but also those of other two periods, are obviously reduced. It is shown that the applied models and the GPS observation data are in better consistency after adding phase residual estimations for ionosphere-free PCVs.

4) The external validation results show that the RMS values of orbit comparison results with JPL precise science orbit and orbit validation results with KBR data in different periods are all obviously reduced. In all periods, the 3D RMS value of orbit comparison results is reduced from 0.059 7 m to 0.055 7 m for GRACE *A* and from 0.056 6 m to 0.054 3 m for GRACE *B*. The standard deviation of KBR validation results is reduced from 0.018 4 m to 0.015 8 m and is comparable to relative position accuracy of JPL precise science orbit.

5) By internal and external validation results, it can be seen that phase residual estimations of current period could not only be used for the calibration for GPS receiver antenna phase center of previous and current periods, but also be used for the forecast of ionosphere-free PCVs in future period, and the accuracy of orbit determination can be well improved.

Acknowledgement

The authors are grateful to GeoForschungsZentrum (GFZ) for providing GPS observation data, attitude data, KBR data and precise science orbit data of GRACE mission. The authors also thank the Center for Orbit Determination in Europe (CODE) for GPS orbit solutions and clock corrections.

References

[1] Reigber Ch, Lühr H, Schwintzer P. CHAMP mission status. Advances in Space Research 2002; 30(2): 129-134.

[2] van den Ijssel J, Visser P, Patiño Rodriguez E. CHAMP precise orbit determination using GPS data. Advances in Space Research 2003; 31(8): 1889-1895.

[3] Kang Z, Nagel P, Pastor R. Precise orbit determination for GRACE. Advances in Space Research 2003; 31(8): 1875-1881.

[4] Kang Z, Tapley B, Bettadpur S, et al. Precise orbit determination for the GRACE mission using only GPS data. Journal of Geodesy 2006; 80(6): 322-311.

[5] Bock H, Jäggi A, Švehla D, et al. Precise orbit determination for the GOCE satellite using GPS. Advances in Space Research 2007; 39(10): 1638-1647.

[6] González J H, Bachmann M, Krieger G. Development of the TanDEM-X calibration concept: analysis of systematic errors. IEEE Transactions on Geosicence and Remote Sensing 2010; 48(2): 716-726.

[7] Hwang Y, Lee B, Kim Y, et al. GPS based orbit determination for KOMPSAT-5 satellite. ETRI Journal 2011; 33(4): 487-496.

[8] Montenbruck O, Ramos-Bosch P. Precision real-time

navigation of LEO satellites using global positioning system measurements. GPS Solutions 2008; 12(3): 187-198.
[9] Wu S, Yunck T, Thornton C. Reduced-dynamic technique for precise orbit determination of low earth satellites. Journal of Guidance Control and Dynamics 1991; 14 (1): 24-30.
[10] Montenbruck O, van Helleputte T, Kroes R, et al. Reduced dynamic orbit determination using GPS code and carrier measurements. Aerospace Science and Technology 2005; 9(3): 261-271.
[11] Beutler G, Jäggi A, Hugentobler U, et al. Efficient satellite orbit modelling using pseudo-stochastic parameters. Journal of Geodesy 2006; 80(7): 353-372.
[12] Montenbruck O, Garcia-Fernandez M, Yoon Y, et al. Antenna phase center calibration for precise positioning of LEO satellites. GPS Solutions 2009; 13(1): 23-34.
[13] Jäggi A, Dach R, Montenbruck O, et al. Phase center modeling for LEO GPS receiver antennas and its impact on precise orbit determination. Journal of Geodesy 2009; 83(12): 1145-1162.
[14] Haines B, Bar-Sever Y, Bertiger W, et al. One-centimeter orbit determination for Jason-1: new GPS-based strategies. Marine Geodesy 2004; 27(1-2): 299-318.
[15] Haines B, Bar-Sever Y, Bertiger W, et al. Space-based satellite antenna maps; impact of different satellite antenna maps on LEO & terrestrial results. IGS Workshop. 2008.
[16] Bock H, Jäggi A, Meyer U, et al. Impact of GPS antenna phase center variations on precise orbits of the GOCE satellite. Advances in Space Research 2011; 47(11): 1885-1895.
[17] Gu D F. The spatial states measurement and estimation of distributed InSAR satellite system. PhD thesis, National University of Defense Technology, 2009. [in Chinese]
[18] Akrour B, Santerre R, Geiger A. Calibrating antenna phase centers. GPS World 2005; 16(2): 49-53.
[19] Zheng W, Houtse H, Zhong M, et al. Effective processing of measured data from GRACE key payloads and accurate determination of Earth's gravitational field. Chinese Journal of Geophysics 2009; 52(8): 1966-1975. [in Chinese]
[20] Case K, Kruizinga G, Wu S. GRACE level 1B data product user handbook Version 1.3. Pasadena: Jet Propulsion Laboratory, 2010.
[21] Dach R, Brockmann E, Schaer S, et al. GNSS processing at CODE: status report. Journal of Geodesy 2009; 83(3-4): 353-365.
[22] Kroes R. Precise relative positioning of formation flying spacecraft using GPS. PhD thesis, Nederlandse Commissie voor Geodetic Commission, 2006.
[23] Tapley B, Ries J, Bettapur S, et al. GGM02—an improved Earth gravity field model from GRACE. Journal of Geodesy 2005; 79(8): 467-478.
[24] McCarthy D D. IERS conventions 1996: IERS technical note 21. Paris: Observatoire de Paris, 1996.
[25] Montenbruck O, Gill E. Satellite orbits. Heidelberg: Springer-Verlag, 2000.
[26] Ferland R. ITRF coordinator report. 2000 IGS Annual Report. Pasadena: Jet Propulsion Laboratory, 2001.
[27] McCarthy D, Petit G. IERS conventions 2003 (IERS technical note 32). Paris: Observetoire de Paris, 2004.
[28] Peng D J, Wu B. Zero-difference and single-difference precise orbit determination for LEO using GPS. Chinese Science Bulletin 2007; 52(15): 2024-2030.
[29] Huang T Y, Zhou Q L. Adams-Cowell integrator with a first sum. Chinese Astronomy and Astrophysics 1993; 17(2): 205-213.

Biographies:

TU Jia is a Ph.D. student at College of Science, National University of Defense Technology. He received the B.S. degree from Qufu Normal University in 2005 and M.S. degree from National University of Defense Technology in 2007. His main research interests are modern statistical theory and precise orbit determination for LEO satellites.
E-mail: tu_jia_jia@yahoo.com.cn

GU Defeng received B.S. and Ph.D. degrees from National University of Defense Technology in 2003 and 2009 respectively, and then became a teacher there. His main research interests are modern statistical method and measurement data processing.
E-mail: gudefeng05@163.com

WU Yi is a professor and Ph.D. supervisor at College of Science, National University of Defense Technology. His current research interests are modern statistical theory and application.
E-mail: wuyi_work@sina.com

YI Dongyun received Ph.D. degree from National University of Defense Technology in 2003. He is currently a professor and Ph.D. supervisor there. His main research interests are dynamic system analysis and measurement data processing.
E-mail: dongyun.yi@gmail.com